Available online at www.sciencedirect.com
SCIENCE DIRECT
Electrochimica Acta 51 (2006) 1815–1819
ELECTROCHIMICA Acta
www.elsevier.com/locate/electacta

Corrosion characterization of titanium alloys by electrochemical techniques

Sérgio Luiz de Assis [a], Stephan Wolynec [b], Isolda Costa [a,*]

[a] *Materials Science and Technology Centre, Institute for Energy and Nuclear Research (IPEN/CNEN-SP), Av. Prof. Lineu Prestes 2242, CEP 05422-970, São Paulo, SP, Brazil*
[b] *Department of Metallurgical and Materials Engineering of the Polytechnic School of the University of São Paulo, Av. Prof. Mello Moraes, 2463, CEP 05508-900, São Paulo, SP, Brazil*

Received 23 June 2004; received in revised form 22 October 2004; accepted 25 February 2005
Available online 24 August 2005

Abstract

The electrochemical behavior of Ti–6Al–4V and Ti–6Al–7Nb alloys, commonly used implant materials, particularly for orthopaedic and osteosynthesis applications, was investigated together with that of Ti–13Nb–13Zr alloy in Hank's solution at 37 °C. The aim of present study was to evaluate their corrosion resistance in an artificial physiological solution. This evaluation was carried out through the analysis of the corrosion potential variation with time, potentiodynamic polarization curves, and electrochemical impedance spectroscopy (EIS) tests. Very low current densities were obtained (order of nA/cm^2) from the polarization curves, indicating a typical passive behavior for all investigated alloys. The EIS results exhibited capacitive behavior (high corrosion resistance) with phase angles close to −90° and high impedance values (order of 10^6 Ω cm^2) at low and medium frequencies, which are indicative of the formation of a highly stable film on these alloys in the test solution. The obtained EIS spectra indicated two relaxation time constants and their interpretation in terms of an "equivalent circuit" with the circuit elements representing the electrochemical properties of a two-layer oxide, composed of a porous outer layer and a dense inner layer, was in good agreement. The electrochemical impedance spectroscopy (EIS) technique, therefore, was able to provide reliable data for determination of the passive film structure.

Keywords: Titanium alloys; Biomaterials; Electrochemical techniques; Corrosion resistance; Osseointegration

1. Introduction

Metallic materials are being increasingly used in medical applications as implants to restore lost functions or replace organs functioning below acceptable levels. Titanium alloys are among the most used metallic biomaterials, particularly for orthopaedic applications [1,2]. They possess a set of suitable properties for these applications such as low specific weight, high corrosion resistance and biocompatibility [3]. Corrosion resistance is a vital property for this kind of application once physiological fluids are chloride containing solutions, with concentration of approximately 1 wt.% NaCl, homeostatically maintained at 37 °C [4]. Furthermore, corrosion products are largely responsible for limited biocompatibility and can produce undesirable reactions in implant-adjacent tissues. Since corrosion resistance plays a decisive role in determining the successful use of metal alloys as biomaterials, the in vitro evaluation of such parameter represents one of the first stages in the procedure for acceptance of new materials for that purpose.

Ever since the pioneer metal alloys have been used as biomaterials, lack of biocompatibility has been extensively reported and propelled research on improved materials with appropriate mechanical behavior and adequate biocompatibility. The Ti–6Al–4V alloy with (α + β) structure was the first titanium alloy registered as implant material in the ASTM standards (F-136-84) [5]. The Ti–6Al–4V and

* Corresponding author. Tel.: +55 11 3816 9456; fax: +55 11 3816 9370.
E-mail address: icosta@ipen.br (I. Costa).

0013-4686/$ – see front matter © 2005 Elsevier Ltd. All rights reserved.
doi:10.1016/j.electacta.2005.02.121

Ti–6Al–7Nb alloys are among the most commonly used implant materials, particularly for dental, orthopaedic and osteosynthesis applications [1,6,7]. Studies have indicated that vanadium, used to stabilize the β-phase, produces oxides harmful to the human body [8,9]. The toxicity of vanadium has pushed forward the search for materials to replace Ti–6Al–4V [5,6]. In order to replace vanadium containing Ti alloys, Ti–6Al–7Nb alloy was developed and this alloy is now commercially available. Niobium is a β–phase stabilizer [7]. Moreover there has been also concern, not yet confirmed, about the association between Al and Alzheimer disease [10,11]. More recently the Ti–13Nb–13Zr, a near β phase alloy, was developed [6]. This alloy contains three of the four elements (Ti, Nb, Zr and Ta) considered as non-toxic [3,9] and displaying excellent biocompatibility [10].

In this scenario, it is important to investigate the corrosion resistance of fairly new Ti-alloys, as well as to compare it with that of commercial alloys. In the present study, the electrochemical behavior of three Ti alloys, specifically Ti–6Al–7Nb and Ti–6Al–4V that are commercial alloys, and a laboratory made Ti–13Nb–13Zr alloy was evaluated in Hank's naturally aerated solution, at 37 °C.

2. Materials and methods

The composition of Ti alloys used in this investigation is shown in Table 1.

The near-β Ti–13Nb–13Zr alloy was obtained by arc melting pure (99.9%) Ti and Nb, along with Zr containing 4.5% Hf, under argon, using a non-consumable electrode. The material was then heat-treated at 1000 °C for 1 h for homogenization and water-cooled. The alloy was subsequently cold forged to 6.5 mm in diameter. In this stage, the alloy was heat-treated again [12]. The Ti–6Al–4V alloy (Supra Alloy Inc.) was heat-treated by the manufacturer at 712 °C for 30 min [13], and the Ti–6Al–7Nb was acquired from IMI Titanium Limited England.

The electrodes were prepared by epoxy cold resin mounting of alloys, leaving areas for exposure to the electrolyte of 0.33, 0.22 and 0.25 cm^2, for the Ti–13Nb–13Zr alloy, Ti–6Al–4V and Ti–6Al–7Nb, respectively. The surfaces exposed to the electrolyte were prepared by sequential grinding with silicon carbide paper up to #2000 finishing, followed by mechanical polishing with diamond paste of 1 μm. The corrosion potential, E_{corr}, variation with time was measured since the first minutes of electrodes immersion in Hank's solution. The samples remained immersed for 72 h in Hank's solution, naturally aerated at 37 °C, and the corrosion potential was measured as a function of time, until its variation with time became negligible. The electrochemical impedance spectroscopy (EIS) and the potentiodynamic polarization tests were performed 72 h after immersion. The testing medium was a naturally aerated Hank's solution, whose composition is given in Table 2. This solution was prepared by Instituto Adolpho Lutz, São Paulo, SP, Brazil.

Table 2
Chemical composition of Hank's solution

Component	Concentration (mol/L)
NaCl	0.1369
KCl	0.0054
$MgSO_4 \cdot 7H_2O$	0.0008
$CaCl_2 \cdot 2H_2O$	0.0013
$Na_2HPO_4 \cdot 2H_2O$	0.0003
KH_2PO_4	0.0004
$C_6H_{12}O_6H_2O$	0.0050
Red phenol 1%	0.0071
pH	6.8

A three-electrode cell arrangement was used for the electrochemical measurements, with a saturated calomel reference electrode (SCE) as reference electrode and a platinum wire as the auxiliary electrode. The polarization and EIS tests were carried out in triplicate to evaluate results reproducibility.

Potentiodynamic polarization scans were carried out with a scan rate of 1 mV/s in the range from −800 mV (SCE) to 3000 mV (SCE) using an EG&G273A potentiostat. The EIS tests were accomplished by means of a Solartron Model SI 1255 Frequency Response Analyzer coupled to a Princeton Applied Research (PAR) Model 273A Potentiostat/Galvanostat and controlled by an Electrochemical Impedance Software PAR model 398. The EIS measurements were obtained in potentiostatic mode and at the corrosion potential, E_{corr}, with voltage perturbation amplitude of 10 mV in the frequency range from 100 kHz to 10 mHz, with 6 points per decade. Experiments were performed in naturally aerated conditions and at 37 °C. The temperature was set to 37 °C by immersing 150 mL electrochemical cells in thermostatic bath.

3. Results

The corrosion potentials, E_{corr}, variation with time of immersion of Ti–13Nb–13Zr, Ti–6Al–7Nb and Ti–6Al–4V alloys in Hank's solution at 37 °C, for a period of 56 h are shown in Fig. 1. The initial E_{corr} for the Ti–13Nb–13Zr

Table 1
Chemical composition (wt.%) of Ti–13Nb–13Zr, Ti–6Al–4V and Ti–6Al–7Nb alloys

Alloy	C	H	N	O	Fe	Al	S	Hf	V	Ta	Nb	Zr	Ti
Ti–13Nb–13Zr	0.035	0.011	0.004	0.078	0.085	–	0.001	0.055	–	–	13.18	13.49	Bal.
Ti–6Al–4V	0.024	0.005	0.006	0.18	0.17	6.0	–	–	4.1	–	–	–	Bal.
Ti–6Al–7Nb	0.08	0.009	0.05	0.20	0,25	6.50	–	–	–	0.50	7.50	–	Bal.

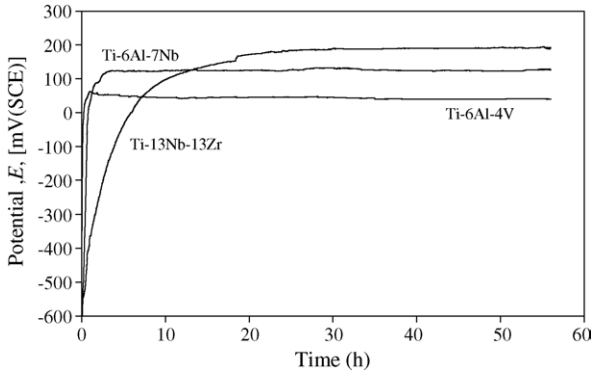

Fig. 1. Corrosion potential, E_{corr}, variation with time curves of Ti–13Nb–13Zr, Ti–6Al–7Nb and Ti–6Al–4V alloys in Hank's naturally aerated solution at 37 °C.

alloy is approximately −560 mV (SCE), and then it gradually increases to nobler potentials reaching after 56 h a steady value at nearly 190 mV (SCE). For the Ti–6Al–7Nb alloy, the initial corrosion potential is around −650 mV (SCE) but it rapidly increased and after approximately 3 h of immersion a value of nearly 120 mV (SCE) was reached. The potential then remained almost constant and after 56 h its value was 127 mV (SCE). The variation of E_{corr} with time for Ti–6Al–4V was similar to that for the Ti–6Al–7Nb alloy. The initial potential is approximately −360 mV (SCE), then it increased rapidly and after 2 h it remained stable at approximately 50 mV (SCE). After 56 h the E_{corr} for this alloy was 40 mV (SCE). The potential was fairly stable from 20 h onwards for all tested samples.

Fig. 2 compares typical potentiodynamic polarization curves of the three Ti alloys tested in Hank's naturally aerated solution at 37 °C after being immersed for 72 h. The average corrosion potentials estimated from these curves were −374 mV (SCE), −368 mV (SCE) and −407 mV (SCE), for the Ti–13Nb–13Zr, Ti–6Al–7Nb and Ti–6Al–4V alloys, respectively.

The corrosion potentials determined from the polarization curves are significantly lower than those obtained from the open circuit potential measurements. This is expected, as the

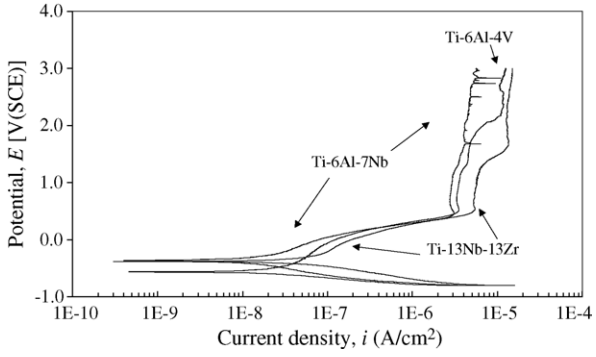

Fig. 2. Potentiodynamic polarization curves for Ti–13Nb–13Zr, Ti–6Al–7Nb and Ti–6Al–4V alloys after 72 h of immersion in Hank's naturally aerated solution at 37 °C. Scanning rate: 1 mV/s.

Table 3
Average values of E_{corr} and i_{corr} determined for the three titanium alloys from the polarization curves obtained in naturally aerated Hank's solution at 37 °C

Alloy	E_{corr} (mV (SCE))	I_{corr} (nA/cm^2)
Ti–13Nb–13Zr	−374 ± 18	28 ± 16
Ti–6Al–4V	−407 ± 28	19 ± 0.9
Ti–6Al–7Nb	−368 ± 8	53 ± 18

polarization test were started at a cathodic potential relatively to the corrosion potential, so that the passive film at the surface was at least partially removed due to the highly reducing initial potentials.

The corrosion current densities (i_{corr}) were obtained from the polarization curves by extrapolation of the cathodic branch of the polarization curves to the corrosion potential, and the mean values and their standard deviation are shown in Table 3. The very low i_{corr} values obtained for the three tested Ti alloys are typical of passive materials.

In the range from corrosion potential to approximately 500 mV (SCE) the polarization curves of all three Ti alloys are S shaped. At approximately 2×10^{-8} A/cm^2 the potential for Ti–6Al–7Nb and Ti–6Al–4V alloys starts to increase faster, and then resumes a slower growth at about 0.0 V (SCE). For Ti–13Nb–13Zr this faster increase starts at about 8×10^{-8} A/cm^2, but the resume of slower growth occurs at approximately the same potential as for the other two alloys. This behavior of all three curves, characterized by a partial stabilization of current density, suggests that in this range of potentials a very protective passive film is formed. This is in agreement with the very low i_{corr} values displayed in Table 3. However, at potentials above approximately 0.0 V (SCE) the sharp increase in current density suggests that this film is gradually replaced by a less protective passive film, which becomes stable above approximately 500 mV (SCE). This film is characterized by passive current densities (i_{pp}) of the order of 3–5 μA/cm^2. In Fig. 2 the lowest i_{pp} is displayed by Ti–6Al–7Nb alloy (at about 3 μA/cm^2), the intermediate value is displayed by the Ti–6Al–4V alloy (at about 3.5 μA/cm^2), and the largest by the Ti–13Nb–13Zr alloy (at about 5 μA/cm^2).

For Ti–13Nb–13Zr alloy the current density starts to increase at approximately 1200 mV (SCE) and then stabilizes again at a current density of about 10^{-5} A/cm^2. Similar increase is observed to occur also for Ti–6Al–4V alloy, but at potentials of the order of 2000 mV (SCE). In this case the current density stabilizes at a value slightly lower than for the previous alloy. For Ti–6Al–7Nb alloy this type of increase is not observed, but some current density oscillations are seen at potentials above 1500 mV (SCE), which could suggest passive film breakdown, in a way similar to that occurring during pitting nucleation and repassivation.

The results of EIS tests are presented through Bode diagrams. These diagrams for the three Ti alloys after 72 h in Hank's solution at 37 °C are shown in Fig. 3. A highly capacitive behavior, typical of passive materials, is indicated from

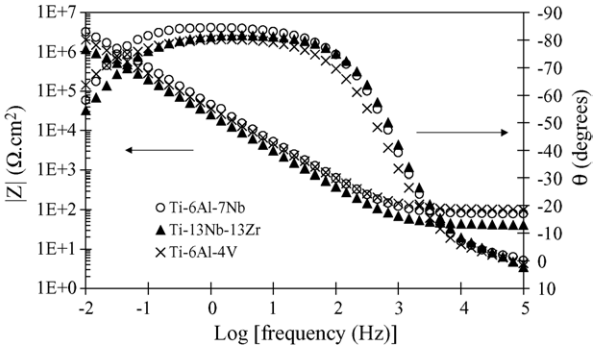

Fig. 3. Bode spectra for Ti–13Nb–13Zr, Ti–6Al–7Nb and Ti–6Al–4V alloys after 72 h in naturally aerated Hank's solution at 37 °C, obtained at the E_{corr}.

medium to low frequencies by phase angles approaching −90°, suggesting that a highly stable film is formed on all tested alloys in the electrolyte used. This is consistent with the very low corrosion rates determined in polarization tests (Table 3).

The large phase angle peak could be indicative of the interaction of at least two time constants. According to literature [14–16] the film on Ti alloys is composed of a bi-layered oxide consisting of a porous outer layer and a barrier inner layer. In work performed by Lavos-Valereto et al. [16] with Ti–6Al–7Nb alloy, in Hank's solution, two relaxation time constants were clearly indicated by two peaks on phase angle plots. Based on these facts the obtained spectra were interpreted in terms of an "equivalent circuit", shown in Fig. 4a. This equivalent circuit is similar to that proposed by Mansfeld and Kendig to represent the oxide layer on anodized aluminum [17] and by Pan et al. [18] for titanium immersed in saline solution. Fig. 4 also shows the experimental data and the fitting for the Ti alloys tested.

The model assumes that the oxide layer on the Ti alloys consists of a barrier-like inner layer and a porous outer layer. In this model, R_s corresponded to the resistance of the solution, R_p to the resistance of the porous layer, R_b to the resistance of the barrier layer, C_p to the capacitance of the porous layer and C_b to the capacitance of the barrier layer. A constant-phase element representing a shift from the ideal capacitor was used instead of the capacitance itself, for simplicity.

The impedance of a phase element is defined as $Z_{CPE} = [C(jw)^n]^{-1}$, where $-1 \leq n \leq 1$. The value of n is associated with the non-uniform distribution of current as a result of roughness and surface defects. The resistance, capacitance and n values of the porous and barrier layers, obtained by

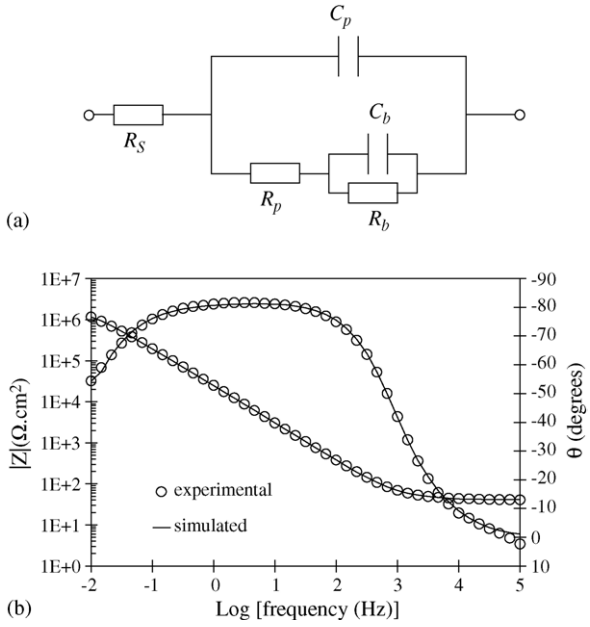

Fig. 4. (a) Equivalent circuit used to adjust experimental data and (b) experimental results and simulated data for Ti–13Nb–13Zr alloy after 72 h in Hank's naturally aerated solution at 37 °C.

adjusting the experimental data using the "equivalent circuit" illustrated in Fig. 4a are given in Table 4. The n values of nearly one suggest that the behavior of such layer approached that of an ideal capacitor [16]. The impedance results were interpreted using the Z_{View} software and the equivalent circuit shown in Fig. 4a. The fitting quality was evaluated by the chi-squared (χ^2) values, which were of the order of 10^{-3}, and the error percentages corresponding to each component of the equivalent circuit (values given in Table 4) indicating that the data adjusted well to the proposed equivalent circuit. This is also indicated in Fig. 4b for the Ti–13Nb–13Zr alloy, where the experimental and the simulated data, according to the proposed circuit, are overploted. Similar fittings were obtained for the other two Ti alloys used in this investigation.

4. Discussion

The analysis of obtained results in all performed electrochemical tests indicates that all tested Ti alloys behaved in a very similar way. The differences are rather small, and this can be ascribed to the fact that the passive film formed on these alloys is essentially of the same nature, that is, it is formed by a titanium oxide, possibly TiO_2. Thus, it can be

Table 4
Electrical parameters of equivalent circuit obtained by fitting the experimental results of EIS

Alloy	R_s (Ω cm²)	C_p (μF cm²)	n	R_p (Ω cm²)	C_b (μF cm²)	n	R_b (MΩ cm²)	χ^2
Ti–13Nb–13Zr	42 (0.4)	2.7 (1.5)	0.98	38 (9.7)	5.1 (1.1)	0.86	2.4 (2.1)	7E-4
Ti–6Al–4V	101 (0.2)	3.4 (1.1)	0.95	287 (10.3)	1.9 (2.3)	0.94	6.4 (2.4)	3E-4
Ti–6Al–7Nb	80 (0.6)	2.9 (2.7)	0.92	478 (16.7)	0.9 (11.2)	0.84	6.6 (4.7)	2E-3

The error percentage resulting from fitting for each component of the equivalent circuit proposed is indicated in parentheses.

expected that in terms of corrosion resistance and osseointegration ability the Ti–13Nb–13Zr implants should have the same performance as those made with the other two alloys.

The corrosion potential curves shown in Fig. 1 indicate that the potential of the Ti alloys in the Hank's solution at 37 °C increases rapidly with time and this initial increase seems to be related to the thickening of the oxide film improving its corrosion protection ability [19].

The very low current densities (order of 10^{-8} A/cm^2) obtained previous to the establishment of a typical passive behavior above 500 mV (SCE), could suggest a direct transition from the immunity region to the passive region [19]. The increase in current density with potential could occur if the increase in potential is not accompanied by a corresponding thickening of the oxide film, or could be due to the oxidation of TiO or Ti_2O_3 to TiO_2 [20]. Nevertheless, it appears that the film formed above 500 mV (SCE) is different from that formed below this potential. Its higher i_{pp} value indicates that it is a more defective oxide. It has been previously proposed that the increase in current density observed at potentials above 1200 mV (SCE) could be related to the formation of Ti compounds such as $NaTiPO_4$ [21].

High impedance values (order of $10^6\,\Omega\,cm^2$) were obtained from medium to low and frequencies for all Ti alloys suggesting, high corrosion resistance in the electrolyte used. This result supports the passive behavior of the alloys, indicated by the polarization curves and the corrosion potential variation with time curves.

The Bode diagrams showing phase angles approaching −90° indicate a highly capacitive behavior typical of a compact passive film [22]. According to the proposed model, the passive film consists of two layers, the inner barrier layer, whose resistance values, R_b, are significantly larger than the values associated to the outer porous layer, R_p. as Table 4 shows. These results indicate that the protection provided by the passive layer is predominantly due to the barrier layer. It has been previously proposed that while the corrosion resistance of the Ti–6Al–7Nb alloy is ascribed to the barrier layer, the ability to osseointegrate should be attributed to the presence of the porous layer [16].

5. Conclusions

The electrochemical techniques used in this investigation led to the following conclusions. Very low corrosion current densities were obtained for the three titanium alloys tested in Hank's solution showing that they are passive in this electrolyte. The EIS results indicated that the film formed on the Ti alloys is composed of a bi-layered oxide consisting of an inner barrier layer associated to high impedance and responsible for corrosion protection, and an outer porous layer, of lower impedance, which apparently facilitates the osseointegration.

References

[1] C. Sittig, M. Textor, N.D. Spencer, M. Wieland, P.-H. Vallotton, J. Mater. Sci : Mater. Med. 10 (1999) 35.
[2] K. Wang, Mater. Sci. Eng. A213 (1996) 134.
[3] M. Niinomi, D. Kuroda, K. Fukunaga, M. Morinaga, Y. Kato, T. Yashiro, A. Suzuki, Mater. Sci. Eng. A263 (1999) 193.
[4] K.J. Bundy, in: R. Baboian (Ed.), Corrosion Tests and Standards: Application and Interpretation, ASTM, Philadelphia, PA, 1995, p. 411.
[5] T. Akahori, M. Niinomi, Mater. Sci. Eng. A243 (1998) 237.
[6] D. Kuroda, M. Niinomi, M. Morinaga, Y. Kato, T. Yashiro, Mater. Sci. Eng. A243 (1998) 244.
[7] M.A. Khan, R.L. Williams, D.F. Williams, Biomaterials 20 (1999) 631.
[8] M.A. Khan, R.L. Williams, D.F. Williams, Biomaterials 17 (1996) 2117.
[9] T.-I. Kim, J.-H. Han, I.-S. Lee, K.-H. Lee, M.-C. Shin, B.-B. Choi, Bio-Med. Mater. Eng. 7 (1997) 253.
[10] Y. Okazaki, Y. Ito, K. Kyo, T. Tateishi, Mater. Sci. Eng. A213 (1996) 138.
[11] S. Rao, Y. Okazaki, T. Tateishi, T. Ushida, Y. Ito, Mater. Sci. Eng. C 4 (1997) 311.
[12] S.G. Schneider, Ph. D. thesis, University of Sao Paulo, Instituto de Pesquisas Energeticas e Nucleares, Brazil (2001).
[13] I. Ramires, A.C. Guastaldi, Quim. Nova 25 (2002) 25.
[14] M.R. Souto, M.M. Laz, R.L. Reis, Biomaterials 24 (2003) 4213.
[15] R. Venugopalan, J.J. Wiemer, M.A. George, L.C. Lucas, Biomaterials 21 (2000) 1669.
[16] I.C. Lavos-Valereto, S. Wolynec, I. Ramires, A.C. Guastaldi, I. Costa, J. Mater. Sci. : Mater. Med. (2004) 55.
[17] F. Mansfeld, M.W. Kendig, J. Electrochem. Soc. 135 (1988) 828.
[18] J. Pan, D. Thierry, C. Leygraf, Electrochem. Acta 41 (1996) 1143.
[19] I.C. Lavos-Valereto, I. Costa, S. Wolynec, J. Biomed. Mater. Res. 63 (2002) 664.
[20] S.Y. Yu, J.R. Scully, Corrosion 53 (1997) 965.
[21] D.M. Considine, in: DM. Considine (Ed.), Van Nostrand's Scientific Encyclopedia, fifth ed., Van Nostrand, New York, 1976, pp. 2210–2212.
[22] J.E.G. González, J.C. Mirza-Rosca, J. Electroanal. Chem 471 (1999) 109.